FEATURE ARTICLE

Check for updates

Non-oxidative coupling of methane *via* selective passivized catalysis

Jacob C. Robinson,† Jiaping Weng,† Tobias K. Misicko, [ID] † Natalie Remedies, Daniela S. Mainardi and Yang Xiao [ID] *

Methane activation remains a grand challenge in catalysis science and reaction engineering. Under nonoxidative conditions, this is likely not due to the intrinsic inertness of CH_4 molecules, but because activity must be balanced with selectivity and long-term stability of catalysts. We clarify that the C–H bond dissociation enthalpy (BDE) of methane, while large, is a poor metric for the catalytic reactivity of methane: BDE is a gas-phase quantity that neither dictates the reaction free energy nor the site-specific activation free energy relevant to reaction pathways. Guided by thermodynamic analysis of non-oxidative coupling of methane (NOCM) and kinetic evidence on Pt-based catalysts, we show that rapid deactivation *via* deep dehydrogenation and coking dominates catalytic performance limits. We advance selective passivized catalysis (SPC) as a differentiated catalyst design strategy in which a fraction of overly active sites is deliberately shielded, *ex situ* (*e.g.*, alloying, support modification, geometric confinement) or *in situ* (reaction-induced passivation), to suppress undesired pathways while preserving sites that promote desired products. SPC reconciles activity with stability and has delivered sustained NOCM performance with C_2 selectivities >90% on Pt–Bi/ZSM-5 and stable operation using Pt nanolayers on $Mo_2TiC_2T_x$ MXene. We outline mechanistic scenarios for solely heterogeneous NOCM and highlight *operando* characterization (EPR, MBMS) to resolve radical *vs.* surface-mediated routes. In this Feature Article, we review that selective passivized catalysis provides a rational blueprint to stabilize methane activation and bring NOCM closer to practical relevance.

Institute for Micromanufacturing and Department of Chemical Engineering, Louisiana Tech University, 505 Tech Drive, Ruston, LA 71272, USA.
E-mail: yxiao@latech.edu; Fax: +1 318-257-4000; Tel: +1 318-257-5109
† These authors contributed equally.

1 Introduction

Methane (CH_4) is the most abundant hydrocarbon on Earth and in the universe.[1–5] Accordingly, its activation into value-added chemicals and fuels has attracted widespread interest in both academia and industry. Two broad strategies have emerged: indirect conversion, which proceeds through methane

Jacob C. Robinson is a PhD student in Chemical Engineering at Louisiana Tech University (LaTech). He received his BS in Chemical Engineering from LaTech in 2024. His research focuses on the design and modeling of catalytic systems for the conversion of short alkanes.

Jacob C. Robinson

Jiaping Weng is a PhD student in Chemical Engineering at LaTech. He received his BS in Environmental Engineering from Changzhou University (China) in 2024. His research focuses on computational catalysis using density functional theory (DFT) and molecular dynamics (MD) simulations to understand the structure–property relationships of novel catalytic materials.

Jiaping Weng

reforming to syngas (CO + H$_2$) followed by downstream processes such as Fischer–Tropsch synthesis (FTS) to produce methanol, ethanol, gasoline, or diesel; and direct conversion, seeking to transform methane into higher-value products without the syngas intermediate.[6–11] Indirect methane conversion refers to pathways where methane carbon is first converted into syngas (CO + H$_2$), which can then be upgraded to fuels and chemicals. Steam reforming of methane is the dominant industrial process, and while its global significance is often framed in terms of hydrogen production, it simultaneously represents the most important indirect carbon utilization pathway. To date, only indirect conversion has achieved industrial significance, with steam reforming of methane (SRM) remaining the dominant route, accounting for ∼95% of U.S. hydrogen production and ∼66% of global production, according to DOE (Department of Energy) and IEA (International Energy Agency) reports.[12–18]

The direct catalytic activation of methane has been extensively investigated since the 1980s.[19–21] However, despite decades of effort, no direct route has achieved successful commercialization, largely due to fundamental challenges of activity selectivity, stability, and thermodynamic limitation of methane activation. The C–H bond in CH$_4$ looks strong

Tobias K. Misicko is the Phillip J. Coane Distinguished PhD candidate in Chemical Engineering at LaTech and a U.S. Department of Energy Office of Science Graduate Student Research (SCGSR) Fellowship awardee. He received his BS in Chemical Engineering from Purdue University in 2022. His research focuses on structure–activity relationships in nanolayer catalysts for the catalytic conversion of short alkanes. He also serves as a Visiting SCGSR Fellow in the Advanced Nuclear Materials Group at Oak Ridge National Laboratory and has been recognized as a Tier I Scholar and past president of LaTech's College of Engineering and Science Graduate Student Council.

Tobias K. Misicko

Natalie Remedies is an undergraduate student majoring in Chemistry at LaTech. She will receive her BS in 2027. Her research focuses on the fundamentals of heterogeneous catalysis. Her recent honors include recognition as a President's Honors Scholar (2025) and recipient of the Mattie Black Gason Memorial College of Engineering and Science Scholarship (2025).

Natalie Remedies

Dr Daniela S. Mainardi is the Thomas and Nelda Jeffery Endowed Professor of Chemical Engineering and Associate Dean of Graduate Studies in the College of Engineering and Science at LaTech. She received her BS in Physics from the University of Buenos Aires, Argentina (1997), MS in Materials Science and Technology from the University of San Martín, Argentina (1998), and PhD in Chemical Engineering from the University of South Carolina (2003). She has specialized in multi-scale modeling of kinetics and thermodynamic processes at the nano-scale with applications to catalysis and energy. Mainardi was awarded the NSF-CAREER award in 2005, among other currently funded awards, she is a Co-Principal Investigator of the largest (up to US$160 million for 10 years) NSF-funded (2024) "FUEL: Future Use of Energy in Louisiana" Cooperative Agreement ever awarded to the state of Louisiana.

Daniela S. Mainardi

Dr Yang Xiao is an Assistant Professor of Chemical Engineering at Louisiana Tech University (LaTech). He received his BS (2010) and PhD (2015) in Chemical Engineering from Southeast University (China), where he conducted joint doctoral research at Purdue University, West Lafayette, IN (2012–2015). He leads the Reaction Engineering & Catalysis Science Laboratory (RECSL), focusing on heterogeneous catalysis, reaction engineering, and multiscale modeling—particularly Selective Passivized Catalysis (SPC) for converting short alkanes into value-added chemicals and fuels. His recent honors include the U.S. NSF Engineering Research Initiation Award (2024), the ACS PRF Doctoral New Investigator Award (2025), and LaTech's Early Career Excellence in Research Award (2025).

Yang Xiao

(bond dissociation enthalpy at 298 K–439 kJ mol^{-1}),[22] while methane activation is often mischaracterized solely in terms of this bond strength. However, we believe that bond dissociation enthalpy (BDE) does not determine the thermodynamic feasibility of catalytic transformations, nor does it represent the kinetic barrier, which is governed by site-specific activation energies (E_a). Among direct routes, oxidative coupling of methane (OCM) has been most extensively studied, producing C$_2$ hydrocarbons such as ethane (C$_2$H$_6$) and ethylene (C$_2$H$_4$). Yet OCM remains plagued by over-oxidation, which restricts C$_2$ yields to only 25–30% even at elevated temperatures ($\sim$800 °C).[8,23,24] Under non-oxidative conditions, two major pathways have been investigated: dehydroaromatization of methane (DHA), which yields aromatics and hydrogen,[25,26] and non-oxidative coupling of methane (NOCM), which targets C$_2$ hydrocarbons and hydrogen.[27] Both DHA and NOCM reactions are highly endothermic, operate at temperatures as high as 700–800 °C, and may be limited by unfavorable equilibrium. Moreover, they suffer from rapid catalyst deactivation driven by sintering and coke deposition.

We recently developed two classes of catalysts for methane activation, particularly in NOCM: Pt–Bi bimetallic catalysts[28] and Pt nanolayer/Mo$_2$TiC$_2$T$_x$ MXene catalysts.[29] These discoveries inspired the concept of selective passivized catalysis (SPC), a new catalyst design strategy in which a portion of active sites is deliberately shielded to suppress side reactions while preserving the activity, selectivity, and stability of the remaining sites. In this Feature Article, we highlight how SPC offers a rational pathway to address the grand challenge of NOCM, achieving stable methane conversion by enabling the first C–H bond activation while simultaneously suppressing deep dehydrogenation and coke formation, and maintaining highly dispersed active sites under harsh reaction conditions.

2 Thermodynamic analysis

2.1 Beyond bond dissociation enthalpy (BDE)

The terms bond dissociation enthalpy (BDE), bond dissociation energy (D_0), and bond energy are often used interchangeably in the methane activation literature, but they are distinct. BDE is the enthalpy change associated with the homolytic cleavage of a specific bond in the gas phase at a given temperature (BDE$_T$).[22,30] D_0 refers to the bond dissociation energy at 0 K, defined as the ground-state electronic energy plus zero-point energy (ZPE); thus, BDE$_0$ and D_0 are equivalent. In contrast, bond energy is the average of all BDE values in a molecule.[31] The common assertion that methane activation is difficult solely because of its high C–H BDE (BDE$_{298K} \approx$ 439 kJ mol^{-1}) is misleading for three reasons as follows: (1) BDE strictly describes homolytic cleavage in the gas phase and does not represent the surface-assisted pathways relevant to heterogeneous catalysis. (2) The BDE of a single bond does not capture the overall thermodynamics of a chemical reaction, which depends on the bond energies of both broken and newly formed bonds. (3) BDE is not a kinetic parameter and should

not be used as a substitute for the activation free energy ($\Delta G^{\ddagger}$), except in limited cases such as homogeneous methane activation.

The appropriate thermodynamic metric for methane activation is the Gibbs free energy change (ΔG_{rxn}), which accounts for both enthalpic and entropic contributions at the reaction temperature. While BDE values can approximate the enthalpy of reaction (ΔH_{rxn}), they are only one part of ΔG_{rxn}, which ultimately dictates spontaneity. Reactivity is instead determined by the site-specific $\Delta G^{\ddagger}$, which reflects the catalytic environment and transition-state stabilization. Only in special cases where homolytic C–H bond cleavage is the rate-determining step—such as gas-phase methane pyrolysis—does the activation energy (312–450 kJ mol^{-1}) closely match the methane C–H BDE.[32–39] By contrast, Lane and Wolf reported an activation energy of only 228 kJ mol^{-1} for homogeneous oxidative coupling of methane,[40] far below the C–H BDE. Thus, methane's large bond dissociation enthalpy is relevant only in limited gas-phase contexts, but it should not be treated as a universal descriptor of catalytic methane reactivity. This distinction is illustrated in Fig. 1(a), where the energy profiles for methane activation are compared. While the gas-phase C–H bond dissociation enthalpy (BDE) lies far above the reaction free energy (ΔG_r) for 2CH$_4$ → C$_2$H$_6$ + H$_2$, the effective barriers on Pt nanoparticles and under selective passivized catalysis (SPC) fall between these extremes. This further supports that BDE alone is not a reliable descriptor of catalytic methane activity, because BDE represents only the enthalpic cost of homolytic bond cleavage in the gas phase. Importantly, the BDE of methane (ca. 439 kJ mol^{-1}) is intrinsically much higher than the experimentally observed activation energies for catalytic methane activation, which typically range between 100–250 kJ mol^{-1}. In heterogeneous catalysis, kinetics, surface chemistry, and entropy contributions play decisive roles, and descriptors such as activation energy and Gibbs free energy changes provide a more complete picture of reactivity. Therefore, while BDE is useful for comparison, it cannot serve as a standalone predictor of methane activation performance.

2.2 Thermodynamic analysis of NOCM

As described in (Rxn. 1) and (Rxn. 2), two C$_2$ species, i.e., C$_2$H$_6$ and C$_2$H$_4$ are the main desired products from nonoxidative coupling of methane (NOCM). After three terms of bond dissociation enthalpy (BDE), bond dissociation energy (D_0), and bond energy have been clarified, thermodynamic analysis needs to be discussed to establish the base line of NOCM.

$$2CH_4 \rightarrow C_2H_6 + H_2 \qquad \text{(Rxn. 1)}$$

$$2CH_4 \rightarrow C_2H_4 + 2H_2 \qquad \text{(Rxn. 2)}$$
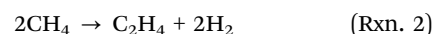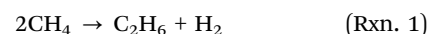
$$\Delta G_{rxn} = \Delta H_{rxn} - T\Delta S_{rxn} \qquad (1)$$

Both reactions are endothermic, with ΔH_{rxn}° = 65.0 kJ mol^{-1} for (Rxn. 1) and ΔH_{rxn}° = 201.5 kJ mol^{-1} for (Rxn. 2), consistent with reported values in Ruscic[22] and Blanksby & Ellison.[30] The corresponding Gibbs free energy changes under standard
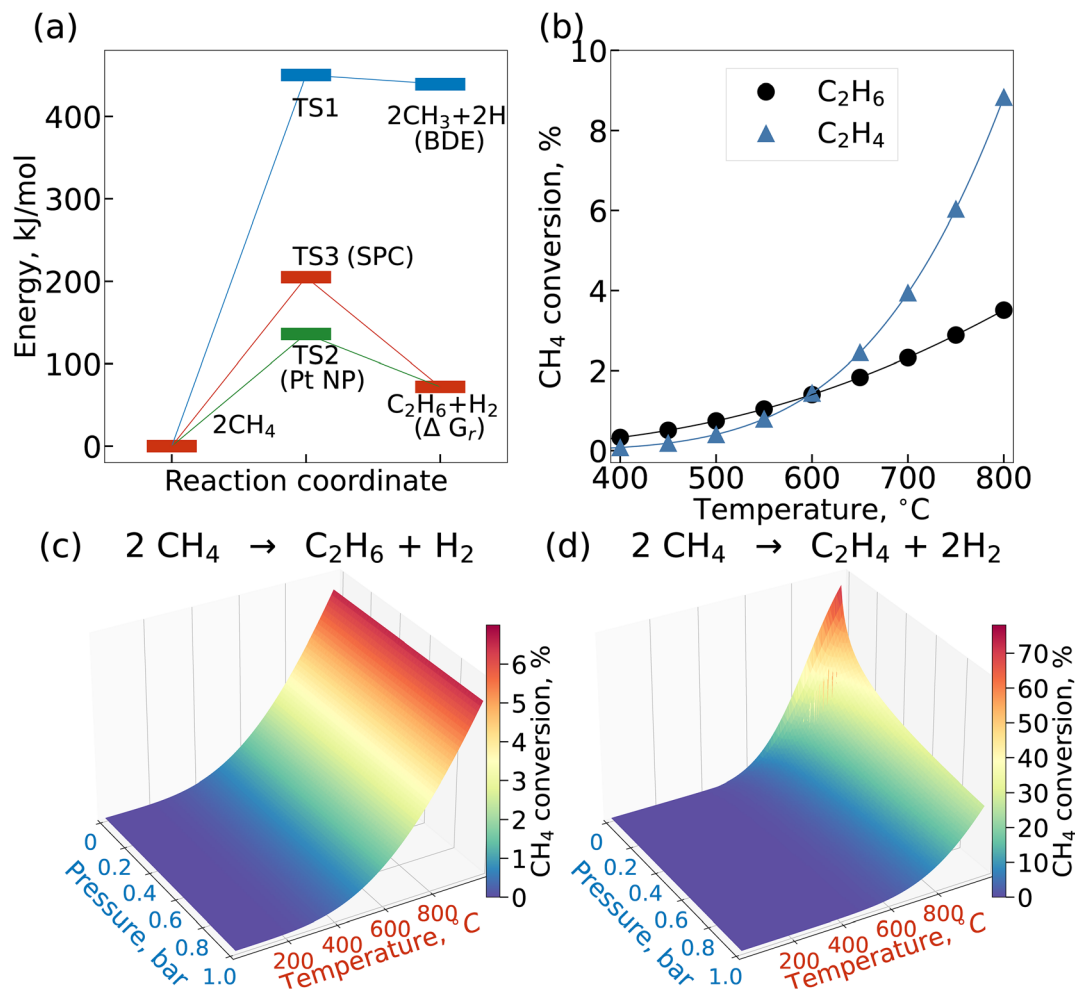
Fig. 1 Thermodynamic analysis in non-oxidative methane coupling (NOCM). (a) Comparison of energy profiles starting from 2CH$_4$, showing the gasphase C–H bond dissociation enthalpy (BDE), the reaction free energy ΔG_r for 2CH$_4 \rightarrow$ C$_2$H$_6$ + H$_2$, and the effective barriers over Pt nanoparticles (Pt NP) and under selective passivized catalysis (SPC); (b) equilibrium conversions of CH$_4$ to C$_2$H$_6$ and C$_2$H$_4$ as a function of temperature at 1 bar CH$_4$ pressure; (c) three-dimensional (3D) plot of CH$_4$ conversion to C$_2$H$_6$ as a function of temperature and pressure; and (d) 3D plot for CH$_4$ conversion to C$_2$H$_4$ as a function of temperature and pressure. Thermodynamic parameters are taken from Ruscic[22] and Blansby & Ellison,[30] and temperature-dependent properties were calculated using Aspen Plus v14.2.

conditions are $\Delta G^\circ_{\text{rxn}} = 68.9$ kJ mol^{-1} and $\Delta G^\circ_{\text{rxn}} = 169.3$ kJ mol^{-1}, respectively. Temperature-dependent thermodynamic properties were calculated using the Aspen Plus process simulator, v14.2. Thus, under ambient conditions, ethane formation (Rxn. 1) is thermodynamically more favorable than ethylene formation (Rxn. 2). Interestingly, the entropy terms for the two reactions point to very different temperature dependences. For (Rxn. 1), the standard entropy of reaction is slightly negative $\left(\Delta S^\circ_{\text{rxn}} = -0.013 \text{ kJ mol}^{-1} \text{ K}^{-1}\right)$, causing ΔG_{rxn} to increase with temperature and making the reaction progressively less favorable. In contrast, (Rxn. 2) has a positive entropy change $\left(\Delta S^\circ_{\text{rxn}} = +0.108 \text{ kJ mol}^{-1} \text{ K}^{-1}\right)$, so the $-T\Delta S_{\text{rxn}}$ contribution becomes dominant at elevated temperatures, and ΔG_{rxn} decreases accordingly. As a result, there exists a temperature threshold (around 600 °C) where ethylene production becomes more favorable than ethane, consistent with the equilibrium analysis of our prior work. These thermodynamic trends are

further illustrated in Fig. 1(b)–(d). Fig. 1(b) shows that equilibrium conversions to C$_2$H$_6$ and C$_2$H$_4$ both increase with temperature, with C$_2$H$_4$ overtaking C$_2$H$_6$ above ∼600 °C. Fig. 1(c) and (d) highlight the combined effects of pressure and temperature: conversion is strongly promoted by high temperature but suppressed at elevated pressure, particularly for C$_2$H$_4$ formation due to its larger positive reaction entropy.

3 Kinetic analysis, catalyst stability, and reaction mechanism

3.1 Kinetic analysis and catalyst stability for NOCM

While thermodynamics sets the ultimate equilibrium limits of NOCM, the reaction rate is governed in practice by kinetics and catalyst stability. The first C–H bond activation in methane is generally regarded as the rate-determining step, and reported

$$2CH_4 \longrightarrow C_2H_6 + H_2$$
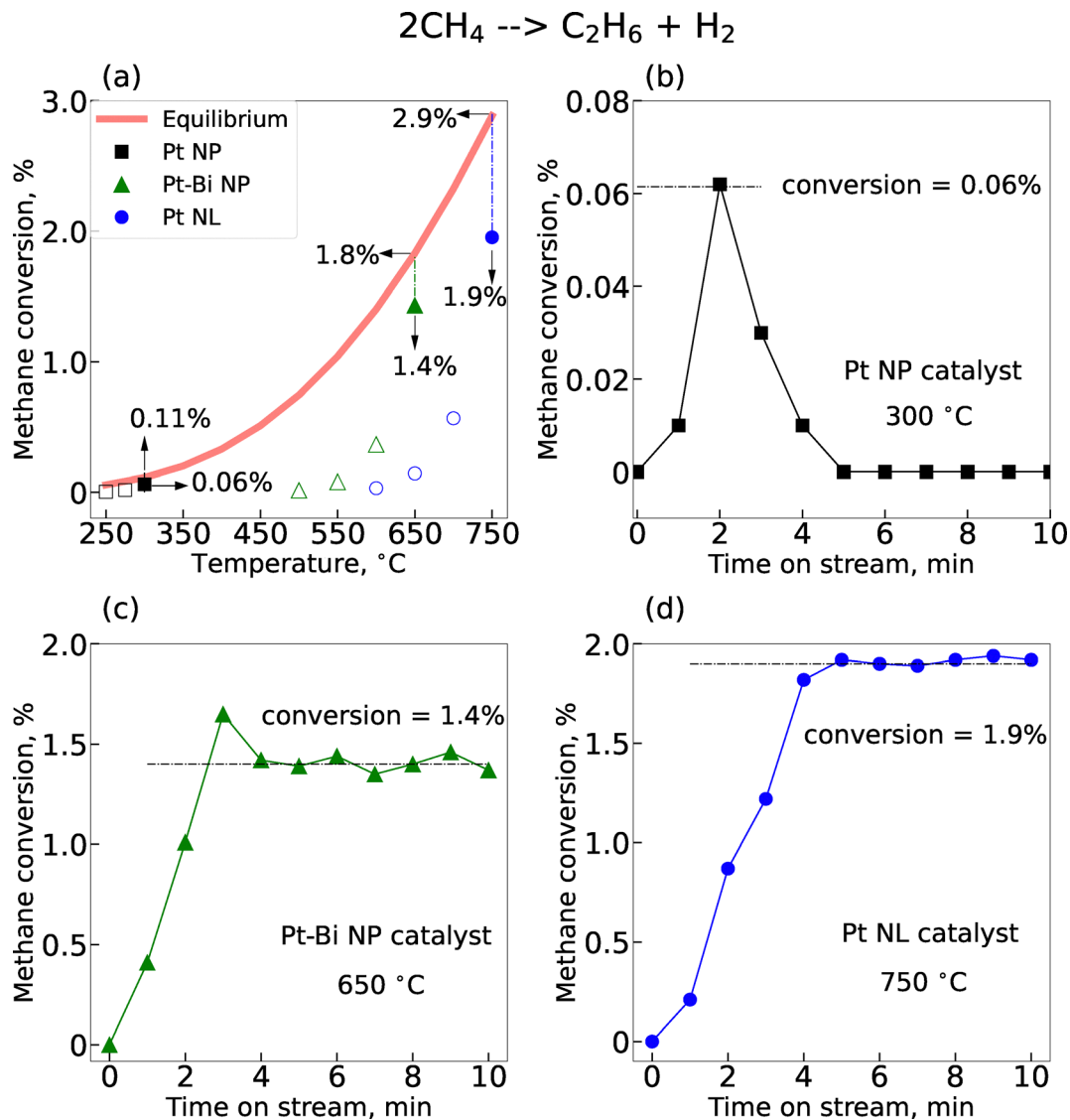
Fig. 2   Kinetic analysis and catalyst stability for NOCM. (a) Equilibrium methane conversions and measured conversions on Pt NP, Pt–Bi NP, and Pt nanolayer (Pt NL) catalysts as a function of temperature. (b) Time-on-stream (TOS) profile for Pt NP at 300 °C, showing rapid deactivation and disappearance of products within ~5 min. (c) TOS profile for Pt–Bi NP at 650 °C, showing stable conversion of 1.4%. (d) TOS profile for Pt NL at 750 °C, showing stable conversion of 1.9%. The equilibrium conversions (0.11% at 300 °C, 1.8% at 650 °C, and 2.9% at 750 °C) are included for comparison.

apparent activation energies vary widely depending on the catalyst. For noble metal catalysts such as Pt, Rh, and Ir, values in the range of 200–350 kJ mol^{-1} have been reported,[41,42] comparable to those measured in gas-phase pyrolysis, but much lower apparent barriers are often observed when surface-mediated pathways dominate. For example, Pt-based catalysts on oxide supports exhibit measurable methane conversion at temperatures as low as 250–300 °C, indicating that catalytic environments can substantially reduce the intrinsic activation energy (Fig. 2(a) and (b)). Fig. 2 was prepared based on our own experimental data for Pt–Bi and Pt nanolayer catalysts,[28,29] combined with reference data for Pt nanoparticles reported by Belgued et al.[41] Catalyst deactivation in NOCM is primarily driven by two phenomena: sintering of metal nanoparticles and severe coke deposition. At elevated temperatures (>600 °C), Pt nanoparticles tend to agglomerate, reducing the density of active sites. More critically, over-activation of CH$_x$ intermediates leads to uncontrolled dehydrogenation and the nucleation of carbon deposits that block active sites and pore structures. These processes result in a precipitous drop in activity within minutes, as observed for Pt/SiO$_2$ catalysts,[41] where initial methane conversion disappears within 5–10 minutes due to coking. Although 200–300 °C is low compared to typical temperatures for bulk coking, surface carbonaceous species can still form under methane-rich, oxygen-free conditions. *Operando* DRIFTS and temperature-programmed oxidation (TPO) studies on Pt/SiO$_2$ catalysts[43] have detected CH$_x$ fragments and oxidizable carbon residues even after short exposures in this temperature range. Similar observations were also reported by Choudhary et al.,[27] where

carbonaceous deposits were detected during non-oxidative methane activation at low temperatures. These findings support that the observed rapid deactivation is indeed coke formation-based, arising from the buildup of highly unsaturated intermediates rather than bulk graphitic carbon.

Nevertheless, sustained reactivity remains challenging, and turnover frequencies (TOFs) often decline rapidly with time-on-stream. Catalyst deactivation in NOCM is primarily driven by two phenomena: sintering of metal nanoparticles and severe coke deposition. At elevated temperatures (>600 °C), Pt nanoparticles tend to agglomerate, reducing the density of active sites. More critically, the over-activation of CH_x intermediates leads to uncontrolled dehydrogenation and the nucleation of carbon deposits that block active sites and pore structures. These processes result in a precipitous drop in activity within minutes, as observed for Pt/SiO_2 catalysts, where initial methane conversion disappears within 5–10 minutes due to coking. Thus, while methane activation itself is not prohibitively slow, the challenge lies in maintaining an active surface under high-temperature and carbon-rich conditions. The catalytic performance of Pt NP, Pt–Bi NP, and Pt nanolayer/Mo_2TiC_2 was presented at 300 °C, 650 °C, and 750 °C, respectively, because each system exhibits stable activity only within its intrinsic temperature window. According to the Arrhenius equation, Pt catalysts are highly active at relatively low temperatures (200–300 °C), but this over-activity also leads to rapid deactivation by coke formation. In contrast, Pt–Bi catalysts require elevated temperatures to reach sufficient activity, while Pt nanolayer catalysts on Mo_2TiC_2 are optimized for stability and selectivity at even higher reaction conditions. Strategies to improve catalyst stability in NOCM have focused on suppressing excessive dehydrogenation and stabilizing active metal dispersion. One approach is the use of site dilution or passivation to reduce ensemble size and minimize coke nucleation. For instance, Pt–Bi bimetallic catalysts reduce the availability (Fig. 2(c)) of contiguous Pt sites, thereby improving resistance to coking and enabling stable operation over hours.[28] Another approach is to confine Pt nanolayers within two-dimensional supports such as Mo_2TiC_2 MXene (Fig. 2(d)), which physically restricts sintering and reshapes the electronic structure of Pt.[29] Both strategies fall under the emerging concept of selective passivized catalysis (SPC), in which a fraction of active sites is intentionally shielded to suppress undesired pathways while retaining activity at the productive sites. In Fig. 2a, solid symbols correspond to the stability tests presented in panels (b), (c), and (d), while hollow symbols denote the activity data collected at lower temperatures for comparison. The long-term stability data underlying the solid symbols are drawn from published studies: Pt–Bi/ZSM-5 catalysts from our earlier ACS Catalysis report,[28] Pt nanolayer/Mo_2TiC_2 catalysts from our Nature Catalysis study,[29] and Pt nanoparticles from Belgued et al.[41] These Pt–Bi and Pt nanoparticles datasets extend to several hours on stream and confirm that SPC-based catalysts can maintain stable operation well beyond the initial time frames highlighted in Fig. 2.

Kinetic evidence for SPC is summarized in Table 1, which compares the apparent activation energies for methane

Table 1 Activation energies (E_a) of methane conversion over Pt nanoparticle (Pt NP), Pt–Bi NP, and Pt nanolayer (Pt NL) catalysts

Catalyst	Pt NP[41]	Pt–Bi NP[28]	Pt NL[29]
E_a, kJ mol^{-1}	136	183	205
Temperature, °C	200–300	500–650	600–750

conversion over Pt nanoparticles (Pt NP), Pt–Bi NP, and Pt nanolayer catalysts. While Pt NP shows a relatively low activation energy (136 kJ mol^{-1}) at 200–300 °C, it rapidly deactivates due to coke formation. In contrast, Pt–Bi NP and Pt NL catalysts exhibit higher apparent activation energies (183 and 205 kJ mol^{-1}, respectively) at elevated operating temperatures, yet maintain stable activity. These results highlight that suppressing over-activation of methane and balancing reactivity with site stability are more critical for sustained NOCM than achieving the lowest possible barrier. In fact, the higher apparent activation energy of Pt–Bi NP (183 kJ mol^{-1}) relative to Pt NP (136 kJ mol^{-1}) reflects the selective passivation of overly active contiguous Pt ensembles by Bi atoms. This passivation suppresses low-barrier coke-forming pathways, leaving only the more selective but higher-barrier routes accessible for methane activation. As a result, the measured activation energy increases, but catalyst stability is greatly improved because deep dehydrogenation and coke nucleation are mitigated. This "high barrier–high stability" relationship illustrates the SPC principle, where slightly reduced intrinsic activity is exchanged for long-term stability and enhanced C_2 selectivity.

3.2 Reaction mechanism of NOCM

The reaction mechanism of non-oxidative coupling of methane (NOCM) remains under active debate. A central question is whether the formation of C–C bonds proceeds through homogeneous gas-phase radical chemistry, similar to oxidative coupling of methane (OCM), or whether it is mediated entirely at the catalyst surface. In OCM, it is well established that CH_4 activation occurs at the catalyst surface, producing CH_3 radicals that enter the gas phase, where they recombine to form C_2 hydrocarbons.[21,44] This heterogeneous–homogeneous mechanism is widely accepted for OCM. In contrast, NOCM may proceed either through a mixed pathway involving gas-phase radicals[27,45] or through a solely heterogeneous mechanism where both C–H activation and C–C coupling occur on the catalyst surface.[28,29] The possibility of a purely heterogeneous mechanism fundamentally distinguishes NOCM from OCM. The recent studies have shown that confinement within two-dimensional MXenes can significantly reshape catalytic pathways. In particular, Pt nanolayers confined on Mo_2TiC_2 MXene have been reported to suppress the release of CH_3 radicals into the gas phase and instead promote surface-mediated C–C coupling routes.[29,45] This interfacial effect provides strong evidence that MXene confinement not only stabilizes Pt ensembles electronically but also limits radical-driven pathways, thereby strengthening the case for a predominantly heterogeneous mechanism in NOCM. At high temperatures

$(T > 1000 \text{ K})$, thermal dissociation of methane can generate gas-phase methyl radicals, as illustrated in eqn (2), which can subsequently couple in the gas phase to form ethane (eqn (3)), followed by stepwise dehydrogenation to ethylene (eqn (4)). This radical-mediated route is well documented,[45] but it carries a significant risk of over-dehydrogenation, leading to coke formation and loss of selectivity.[28] *In situ* characterization has revealed critical insights into how catalysts steer NOCM reactivity. For Pt nanolayers confined within Mo_2TiC_2 MXene, *in situ* XPS and XANES studies confirm strong electronic modification of Pt ensembles, suppressing gas-phase radical release and stabilizing surface-mediated C–C coupling pathways.[29] *Operando* DRIFTS spectra show the presence of CH_x intermediates bound to Pt surfaces, while Raman spectroscopy detects coke precursors only when over-dehydrogenation is not adequately suppressed. Furthermore, molecular beam mass spectrometry (MBMS) and electron paramagnetic resonance (EPR) measurements reported in the literature have directly probed transient methyl radicals, establishing that radical pathways compete but can be suppressed under SPC conditions. These observations underscore that catalyst-induced confinement and ensemble control reshape the distribution of intermediates and radicals, enabling a shift toward selective heterogeneous pathways.

$$CH_4 \rightarrow {}^{\bullet}CH_3 + {}^{\bullet}H \quad (2)$$

$$2{}^{\bullet}CH_3 \rightarrow C_2H_6 \quad (3)$$

$$C_2H_6 \rightarrow C_2H_4 + H_2 \quad (4)$$
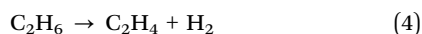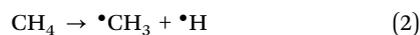
Alternatively, surface-mediated mechanisms propose that both methane activation and C–C coupling occur entirely at the catalyst surface. In this case, CH_4 undergoes dissociative adsorption (eqn (5)) to form chemisorbed methyl species (CH_3^*), which couple on the surface to form C_2 species that can desorb as ethane or undergo further dehydrogenation to ethylene, acetylene, or coke precursors.[27–29]

$$CH_4 + 2^* \rightarrow CH_3^* + H^* \quad (5)$$

$$CH_4 \rightarrow C_2H_6 \rightarrow C_2H_4 \rightarrow C_2H_2 \rightarrow C(s) + H_2 \quad (6)$$
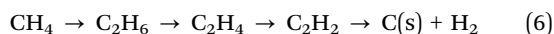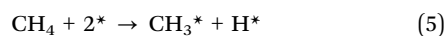
Computational studies, including microkinetic modeling and density functional theory (DFT), provide support for such heterogeneous pathways, with kinetics strongly dependent on the electronic structure and ensemble size of the active surface.[28,46] The key challenge in both cases is over-dehydrogenation of intermediates, which accelerates coke formation (eqn (6)) and limits stability. Inhibiting these side reactions requires precise control over the extent of C–H activation and C–C coupling, as well as strategies that promote rapid desorption of desired products before further conversion. In summary, unlike OCM where a heterogeneous–homogeneous mechanism is well established, NOCM may proceed *via* a solely heterogeneous pathway in which the catalyst surface mediates both activation and coupling. Demonstrating and controlling such a mechanism is critical to achieving high selectivity and stability for C_2 production under non-oxidative conditions.

4 Selective passivized catalysis (SPC)

4.1 Definition of SPC

One of the most pressing challenges in heterogeneous catalysis is catalyst stability,[47–49] which is especially severe for methane activation under oxygen-free conditions.[43,50–52] Over 120 deactivation descriptors have been identified in the literature,[53] including depletion, segregation, poisoning, aggregation, *etc.* Despite its critical importance for industrial deployment, catalyst stability is often treated superficially in academic studies, leaving a major gap between laboratory success and practical application.[54] Catalyst passivation typically refers to post-synthesis treatments that form protective surface layers, often to prevent oxidation during storage or handling.[49,55–57] However, many catalysts suffer from low selectivity and rapid deactivation due to undesired side reactions initiated at highly active sites like steps/corners. To address this, passivation has been applied to suppress such overly active sites, for example, reducing cracking in propane dehydrogenation.[58–61] Yet these measures are often viewed as auxiliary rather than design strategy.

Mo_2TiC_2 belongs to the MXene family of two-dimensional transition metal carbides and carbonitrides, which are typically synthesized by selective etching of the A element (*e.g.*, Al) from MAX phases. It consists of layered Mo–Ti–C slabs terminated by functional groups such as –O, –OH, or –F, which impart hydrophilicity and tunable surface chemistry. Mo_2TiC_2 exhibits high metallic conductivity and strong electronic interactions with supported metals, making it a promising catalyst support. Importantly, it maintains good structural integrity and chemical stability up to $\sim 800\,^{\circ}C$ under inert or reducing conditions, which is suitable for methane activation catalysis.[62,63] Our recent work on Pt nanolayer/Mo_2TiC_2 MXene[29,64] and Pt–Bi catalysts[28,65–69] demonstrates the feasibility and value of elevating passivation to a deliberate and strategic design strategy: selective passivized catalysis (SPC). Here, "passivized" refers to the deliberate design of catalytic surfaces to selectively suppress unproductive active sites—distinguishing it from conventional passivation for surface protection. Selective passivized catalysis is a catalytic design strategy in which a portion of active sites is deliberately shielded, attenuated or modified, either prior to the reaction (*ex situ*) or dynamically during the reaction (*in situ*), to suppress undesired side reactions while retaining high activity and selectivity at the desired sites. The SPC concept is schematically illustrated in Fig. 3, where Bi atoms passivize contiguous Pt ensembles on nanoparticles, and Pt nanolayers confined within Mo_2TiC_2 MXene are stabilized to expose edge ensembles, together suppressing deep dehydrogenation while preserving the active sites required for methane activation and C–C coupling. Note that high-resolution HAADF-STEM and *in situ* XPS measurements of Pt nanolayer/Mo_2TiC_2 MXene catalysts provide direct evidence of selective passivation effects. As reported in Xiao *et al.*,[29] atomically thin Pt nanolayers strongly interact with the MXene support through Pt–Mo bonding, leading to suppressed deep dehydrogenation and resistance to coke deposition. Aberration-corrected TEM
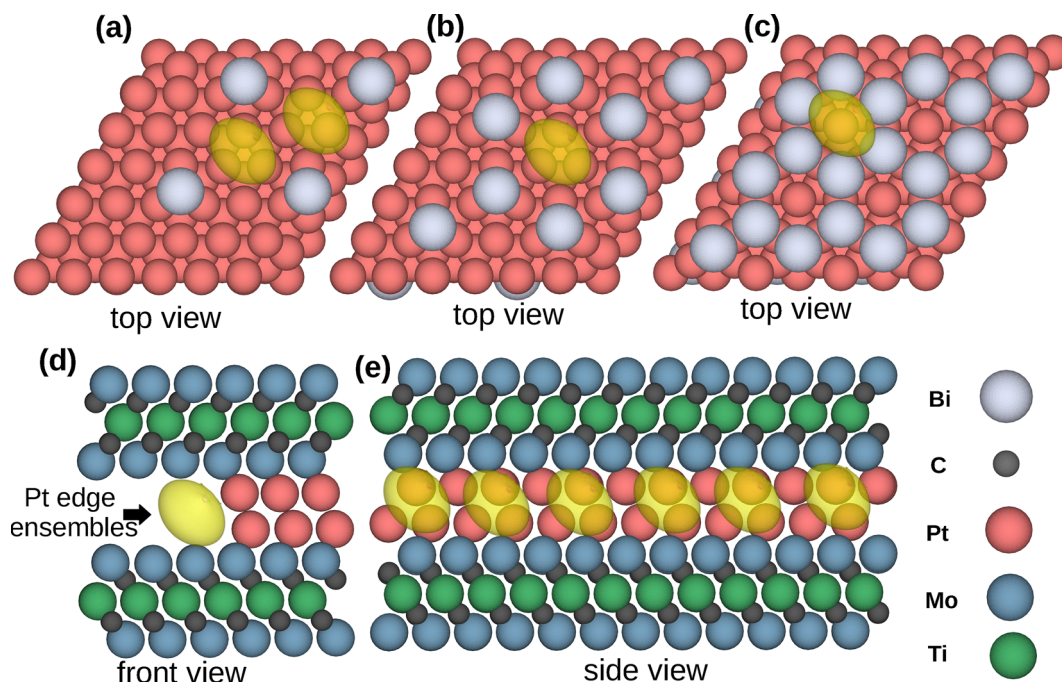
Fig. 3 Schematic illustration of the selective passivized catalysis (SPC) concept. (a)–(c) Top-view models of Pt nanoparticles (Pt NP) with Bi coverages of 0.11, 0.22, and 0.25 monolayers (ML), showing how Bi atoms (grey) selectively block contiguous Pt ensembles (red) to suppress over-activation and coke formation while preserving isolated Pt sites for C–H activation. (d) and (e) Side-view models of Pt nanolayers confined in Mo_2TiC_2 MXene, where the two-dimensional support stabilizes Pt layers and provides edge ensembles that limit deep dehydrogenation. Yellow isosurfaces highlight the active centers involved in methane activation.

images show Pt bilayers stabilized on the MXene basal plane, while in situ XPS and XANES confirm electronic modification of Pt sites that disfavors over-dehydrogenation. This selective site-blocking reduces the absolute activity relative to Pt nano-particles, but significantly improves C_2 selectivity ($>98\%$) and stability (72 h without deactivation at 750 °C). These findings substantiate the SPC concept: passivation of overly active ensembles sacrifices some intrinsic activity while enabling superior performance in terms of selectivity and long-term stability.

4.2 Ex situ SPC and applications in NOCM

A summary of representative SPC catalysts applied in NOCM is provided in Table 2. Both ex situ and in situ strategies are included, highlighting how site passivation through support modification, alloying, confinement, or dynamic restructuring improves C_2 selectivity and stability under diverse operating conditions.

The ex situ SPC refers to strategies where catalyst sites are selectively modified prior to reaction. This may be achieved through physical isolation,[72,73] electronic tuning by alloying or support interactions,[74,75] or geometric confinement.[76–78] The objective is not wholesale deactivation of the catalyst surface, but the targeted suppression of non-selective pathways while preserving reactivity at productive sites. Classical examples include selective passivation of Brønsted acid sites: Bauer et al.[79] suppressed disproportionation and transalkylation in ZSM-5 and FER zeolites by silanization and pre-coking, while maintaining internal acid sites for isomerization. Gan et al.[80] applied a silicalite-1 overlayer to Mo/HZSM-5, blocking external acid sites while retaining internal Mo–C centers and moderated acidity, thereby improving stability in aromatization. Yaluris et al.[58] showed that ammonia pretreatment of sulfated zirconia selectively deactivated the strongest Brønsted acid sites, enhancing stability in n-butane isomerization. These cases illustrate the broader principle of ex situ SPC: targeted site passivation enhances selectivity and catalyst lifetime.

Table 2 Selective passivized catalysts for non-oxidative methane coupling (NOCM)

Active phase	Support	T (°C)	P (atm)	GHSV (ml g_{cat}^{-1} h^{-1})	CH$_4$ conv. (%)	C$_2$ sel. (%)	Ref.
Mo$_2$C (2 wt%)	[B]ZSM-5	650	1	24 000	0.8 (18 h)	90	70
Pt–Sn (1:2)	H-ZSM-5	700	1	2520	0.3 (6 h)	65	60
Pt–Sn (1:3)	H-ZSM-5	700	1	2520	0.1 (8 h)	90	60
Pt (1%)–Bi (0.8%)	ZSM-5	650	1	12 000	2.0 (8 h)	92	28
Pt (0.5 wt%)	Mo$_2$TiC$_2$T$_x$ MXene	750	1	—	3.5–6.5 (72 h)	98	29
Ru–Sn (70:30)	Montmorillonite (Mont)	500	5.9	300	0.15 (3 h)	99	71
Ru–Sn (70:30)	Mesoporous silica–alumina (MS, Si/Al = 30)	500	5.9	300	0.16 (24 h)	99	71

The same principle has been successfully extended to non-oxidative methane coupling (NOCM). Sheng et al.[70] designed a $Mo_2C/[B]ZSM-5$ catalyst, where substitution of B into ZSM-5 reduced Brønsted acidity, suppressing ethylene oligomerization and coke. At 650 °C and 1 atm, $Mo_2C/[B]ZSM-5$ achieved >90% ethylene selectivity and retained 93% of its initial activity after 18 h on stream. Gerceker et al.[60] prepared Pt–Sn catalysts by impregnation, showing that alloying Pt with Sn suppressed dehydrogenation and coke, resulting in higher ethylene TOFs and improved carbon balance relative to Pt/SiO_2. We[28] reported Pt–Bi/ZSM-5 catalysts with ∼2% methane conversion and >90% C_2 selectivity at 650 °C, where Bi functioned as a promoter to enhance C–C coupling and resist coke deposition. Li et al.[29] further advanced the concept by constructing atomically thin Pt nanolayers confined on Mo_2TiC_2 MXene. Kinetic and in situ characterization showed that the nanolayers preferentially activated methane to CH_3* species that desorbed rather than undergoing further dehydrogenation. At 750 °C, these catalysts achieved 7% methane conversion with >98% C_2 selectivity and operated stably for 72 h. These examples demonstrate that ex situ SPC—whether via support modification, alloying, or geometric confinement, enables methane activation while suppressing coke-forming pathways. This approach shifts the design paradigm from maximizing intrinsic activity to balancing reactivity with stability, a prerequisite for practical NOCM.

4.3 In situ SPC and applications in NOCM

In contrast to ex situ strategies, in situ SPC involves dynamic, reaction-induced passivation in which surface species formed during operation evolve into catalytically active sites for the desired reaction.[24,81] Instead of being detrimental, such surface modifications—often originating from coke precursors—can selectively deactivate undesired sites while leaving productive sites intact. The concept parallels commercial processes such as methanol-to-olefins (MTO), where the "hydrocarbon pool" mechanism stabilizes reactivity: an induction period deposits hydrocarbon intermediates on zeolite surfaces, after which activity and selectivity increase.[82] Examples of in situ SPC are emerging across catalytic systems. Gómez-Sanz et al.[83] showed that coke precursors formed during ethylbenzene dehydrogenation selectively passivize Cr^0/Cr^{2+} sites responsible for undesired C–C bond scission, while preserving Cr^{3+} sites active for C–H bond cleavage. This selective passivation maintained high styrene selectivity over extended operation. Similarly, Kromwijk et al.[84] reported that W/ZSM-5 catalysts for methane dehydroaromatization exhibited improved performance after an activation period under methane flow. Operando UV-vis spectroscopy indicated that benzene formation began prior to complete carburization of tungsten oxide, consistent with the buildup of neutral aromatics, hydrocarbon pool intermediates, and polyaromatics during the induction stage. These observations parallel MTO behavior and suggest that pre-coking can enhance methane conversion catalysts.

Our own work further demonstrates in situ SPC in NOCM. By selectively suppressing terrace sites, which is known to drive structure-sensitive coke formation, we achieved 9-day stable methane conversion without deactivation.[29] This strategy reflects a broader principle: modulation of overly active sites by reaction-induced species can stabilize performance by channeling reactivity through productive pathways. Indeed, passivation has long been used to control selectivity in industrial zeolite catalysts for isomerization,[85] MTO,[86] and Exxon's MSTDP process.[81] In all cases, coke or similar surface species act as selective site blockers rather than as poisons. Motokura et al.[71] provided another example by designing a Ru–Sn catalyst that self-assembled into an active bimetallic phase under NOCM conditions. In situ X-ray absorption fine structure (XAFS) analysis revealed that Ru(IV) was first reduced to Ru(0), which activated methane, while hydrogen spillover partially reduced Sn(IV). The resulting Ru–Sn interaction suppressed coke formation, with Sn acting as a selective blocker of coke-forming sites. This illustrates how in situ alloying and passivation can emerge spontaneously during operation to stabilize C_2 production. These examples show that in situ SPC is not merely tolerance of coking, but strategic utilization of reaction-induced surface modifications to enhance selectivity and stability. For NOCM, where overdehydrogenation and coke formation are persistent challenges, in situ SPC represents a promising pathway toward achieving sustained operation without deactivation.

5 Summary and outlook

The grand challenge of non-oxidative methane coupling (NOCM) lies not in the intrinsic difficulty of activating methane, but in balancing activity, selectivity, and catalyst stability. Methane's C–H bond dissociation enthalpy (BDE) is often cited as evidence of its inertness; however, BDE is not a reliable metric for catalytic reactivity. Our studies and others demonstrate that methane can be activated at relatively low temperatures, but rapid catalyst deactivation due to coke formation remains the dominant barrier to practical operation. Thus, the central task is not simply to overcome a high activation barrier, but to design catalysts that suppress dehydrogenation pathways leading to coke while maintaining sufficient activity for productive C–C coupling. Selective passivized catalysis (SPC) has emerged as a promising design concept to address this challenge. Although passivation strategies are not new in catalysis, SPC is differentiated by its deliberate shielding of a fraction of active sites to suppress non-selective pathways while preserving the reactivity of productive sites. This counterintuitive approach, accepting slightly lower intrinsic activity in exchange for improved selectivity and long-term stability, has already shown success in short alkane dehydrogenation and is particularly impactful in NOCM. Ex situ strategies such as alloying, support modification, and geometric confinement, as well as in situ pathways where coke precursors evolve into selective passivating agents, both demonstrate the versatility of SPC in enabling more robust catalytic performance. Examples such as Bi-modified Pt catalysts and Pt nanolayers confined within Mo_2TiC_2 MXene illustrate how SPC can be proactively engineered. Further advances

will depend on deeper mechanistic understanding, including *in situ* and *operando* techniques such as electron paramagnetic resonance (EPR) for radical detection and molecular beam mass spectrometry (MBMS) for gas-phase analysis, combined with *ex situ* tools like time-of-flight secondary ion mass spectrometry (ToF-SIMS) for probing coke species, are well suited to uncover the interplay between surface-mediated and radical-driven pathways. Future engineering of SPC can move beyond empirical trial-and-error approaches by incorporating descriptor-based catalyst design, in which electronic and geometric descriptors guide the rational selection of alloying elements, supports, or confinement structures. Machine-learning-assisted screening combined with DFT can further accelerate identification of promising SPC systems. In addition, *in situ* and *operando* characterization (*e.g.*, DRIFTS, Raman, ToF-SIMS) will provide real-time insights into dynamic site passivation, enabling rational control of SPC under reaction conditions. In conclusion, SPC provides not only a conceptual framework to explain stable methane activation but also a forward-looking strategy to design future catalysts deliberately, bringing NOCM closer to practical relevance.

Conflicts of interest

The authors declare no conflicts of interest.

Data availability

This article does not include new data. All data discussed are from previously published sources, which are cited in the References section.

Acknowledgements

References

1 D. J. Wuebbles and K. Hayhoe, Atmospheric Methane and Global Change, *Earth-Sci. Rev.*, 2002, **57**(3), 177–210.
2 M. Peplow, The Great Gas Gold Rush, *Nature*, 2017, **550**, 26–28.
3 A. Serovaiskii and V. Kutcherov, Formation of Complex Hydrocarbon Systems from Methane at the Upper Mantle Thermobaric Conditions, *Sci. Rep.*, 2020, **10**(1), 4559.
4 N. Sanchez-Bastardo, R. Schlogl and H. Ruland, Methane Pyrolysis for Zero-Emission Hydrogen Production: a Potential Bridge Technology from Fossil Fuels to a Renewable and Sustainable Hydrogen Economy, *Ind. Eng. Chem. Res.*, 2021, **60**(32), 11855–11881.
5 J. Guo, J. Gao, K. Yan, B. Zhang and H. Liu, Castles in the Sky: Revisiting the Global Methane Pledge, *Energy Policy*, 2025, **206**, 114785.
6 R. Horn and R. Schlogl, Methane Activation by Heterogeneous Catalysis, *Catal. Lett.*, 2015, **145**(1), 23–39.
7 Z. Zakaria and S. Kamarudin, Direct Conversion Technologies of Methane to Methanol: An Overview, *Renewable Sustainable Energy Rev.*, 2016, **65**, 250–261.
8 C. Karakaya and R. J. Kee, Progress in the Direct Catalytic Conversion of Methane to Fuels and Chemicals, *Prog. Energy Combust. Sci.*, 2016, **55**, 60–97.
9 W. Taifan and J. Baltrusaitis, CH4 Conversion to Value Added Products: Potential, Limitations and Extensions of a Single Step Heterogeneous Catalysis, *Appl. Catal., B*, 2016, **198**, 525–547.
10 P. Schwach, X. Pan and X. Bao, Direct Conversion of Methane to Value-Added Chemicals over Heterogeneous Catalysts: Challenges and Prospects, *Chem. Rev.*, 2017, **117**(13), 8497–8520.
11 Y. Tang, Y. Li and F. (Feng) Tao, Activation and Catalytic Transformation of Methane under Mild Conditions, *Chem. Soc. Rev.*, 2022, **51**, 376–423.
12 Y. Matsumura and T. Nakamori, Steam Reforming of Methane over Nickel Catalysts at Low Reaction Temperature, *Appl. Catal., A*, 2004, **258**(1), 107–114.
13 R. P. Balegedde Ramachandran, G. van Rossum, W. P. M. van Swaaij and S. R. A. Kersten, Preliminary Assessment of Synthesis Gas Production Via Hybrid Steam Reforming of Methane and Glycerol, *Energy Fuels*, 2011, **25**(12), 5755–5766.
14 R. B. Duarte, F. Krumeich and J. A. van Bokhoven, Structure, Activity, and Stability of Atomically Dispersed Rh in Methane Steam Reforming, *ACS Catal.*, 2014, **4**(5), 1279–1286.
15 H. Zhang, Z. Sun and Y. H. Hu, Steam Reforming of Methane: Current States of Catalyst Design and Process Upgrading, *Renewable Sustainable Energy Rev.*, 2021, **149**, 111330.
16 J. O. Ighalo and P. B. Amama, Recent Advances in the Catalysis of Steam Reforming of Methane (SRM), *Int. J. Hydrogen Energy*, 2024, **51**, 688–700.
17 Hydrogen Program Plan. US Department of Energy. 2024; **https://www.hydrogen.energy.gov/docs/hydrogenprogramlibraries/pdfs/hydrogenprogram-plan-2024.pdf**.
18 Global Hydrogen Review 2024. International Energy Agency. 2024; **https://www.iea.org/reports/global-hydrogen-review-2024**.
19 G. Keller and M. Bhasin, Synthesis of Ethylene Via Oxidative Coupling of Methane: I. Determination of Active Catalysts, *J. Catal.*, 1982, **73**(1), 9–19.
20 D. J. Driscoll, W. Martir, J. X. Wang and J. H. Lunsford, Formation of Gas-Phase Methyl Radicals over Magnesium Oxide, *J. Am. Chem. Soc.*, 1985, **107**(1), 58–63.
21 E. V. Kondratenko and M. Baerns, Oxidative Coupling of Methane, *Handbook of Heterogeneous Catalysis*, 2nd edn, 2008, pp. 3010–3023.
22 B. Ruscic, Active Thermochemical Tables: Sequential Bond Dissociation Enthalpies of Methane, Ethane, and Methanol and the Related Thermochemistry, *J. Phys. Chem. A*, 2015, **119**(28), 7810–7837.
23 E. V. Kondratenko, T. Peppel, D. Seeburg, V. A. Kondratenko, N. Kalevaru, A. Martin and S. Wohlrab, Methane Conversion Into Different Hydrocarbons or Oxygenates: Current Status and Future Perspectives in Catalyst Development and Reactor Operation, *Catal. Sci. Technol.*, 2017, **7**, 366–381.
24 J. Liu, J. Yue, M. Lv, F. Wang, Y. Cui, Z. Zhang and G. Xu, From Fundamentals to Chemical Engineering on Oxidative Coupling of Methane for Ethylene Production: a Review, *Carbon Resour. Convers.*, 2022, **5**(1), 1–14.
25 J. J. Spivey and G. Hutchings, Catalytic Aromatization of Methane, *Chem. Soc. Rev.*, 2014, **43**(3), 792–803.
26 K. Sun, D. M. Ginosar, T. He, Y. Zhang, M. Fan and R. Chen, Progress in Nonoxidative Dehydroaromatization of Methane in the Last 6 Years, *Ind. Eng. Chem. Res.*, 2018, **57**(6), 1768–1789.
27 T. V. Choudhary, E. Aksoylu and D. W. Goodman, Nonoxidative Activation of Methane, *Catal. Rev.*, 2003, **45**(1), 151–203.
28 Y. Xiao and A. Varma, Highly Selective Nonoxidative Coupling of Methane over Pt-Bi Bimetallic Catalysts, *ACS Catal.*, 2018, **8**(4), 2735–2740.

29 Z. Li, Y. Xiao, P. R. Chowdhury, Z. Wu, T. Ma, J. ZhuChen, G. Wan, T. H. Kim, D. Jing, P. He, P. J. Potdar, L. Zhou, Z. Zeng, X. Ruan, J. T. Miller, J. P. Greeley, Y. Wu and A. Varma, Direct Methane Activation by Atomically Thin Platinum Nanolayers on Two-Dimensional Metal Carbides, *Nat. Catal.*, 2021, **4**(10), 882–891.

30 S. J. Blanksby and G. B. Ellison, Bond Dissociation Energies of Organic Molecules, *Acc. Chem. Res.*, 2003, **36**(4), 255–263.

31 P. Muller, Glossary of Terms Used in Physical Organic Chemistry, *Pure Appl. Chem.*, 1994, **66**(5), 1077–1184.

32 G. B. Skinner and R. A. Ruehrwein, Shock Tube Studies on the Pyrolysis and Oxidation of Methane, *J. Phys. Chem.*, 1959, **63**(10), 1736–1742.

33 V. Kevorkian, C. Heath and M. Boudart, The Decomposition of Methane in Shock Waves, *J. Phys. Chem.*, 1960, **64**(8), 964–968.

34 H. B. Palmer and T. J. Hirt, The activation energy for the pyrolysis of methane, *J. Phys. Chem.*, 1963, **67**(3), 709–711.

35 H. B. Palmer, J. Lahaye and K. C. Hou, Kinetics and Mechanism of the Thermal Decomposition of Methane in a Flow System, *J. Phys. Chem.*, 1968, **72**(1), 348–353.

36 R. Hartig, J. Troe and H. Wagner, Thermal Decomposition of Methane behind Reflected Shock Waves, *Symp. (Int.) Combust.*, 1971, **13**(1), 147–154.

37 D. H. Napier and N. Subrahmanyam, Pyrolysis of Methane in a Single Pulse Shock Tube, *J. Appl. Chem. Biotechnol.*, 1972, **22**(3), 303–317.

38 W. Gardiner, J. Owen, T. Clark, J. Dove, S. Bauer, J. Miller and W. McLean, Rate and Mechanism of Methane Pyrolysis from 2000 to 2700 K, *Symp. (Int.) Combust.*, 1975, **15**(1), 857–868.

39 A. Holmen, O. A. Rokstad and A. Solbakken, High-Temperature Pyrolysis of Hydrocarbons. 1. Methane to Acetylene, *Ind. Eng. Chem. Process Des. Dev.*, 1976, **15**(3), 439–444.

40 G. S. Lane and E. E. Wolf, Methane Utilization by Oxidative Coupling: I. A Study of Reactions in the Gas Phase during the Cofeeding of Methane and Oxygen, *J. Catal.*, 1988, **113**(1), 144–163.

41 M. Belgued, P. Pareja, A. Amariglio and H. Amariglio, Conversion of Methane into Higher Hydrocarbons on Platinum, *Nature*, 1991, **352**, 789–790.

42 F. Solymosi, G. Kutsan and A. Erdohelyi, Catalytic Reaction of CH4 with CO2 over Alumina-Supported Pt Metals, *Catal. Lett.*, 1991, **11**(2), 149–156.

43 A. D. Talpade, G. Canning, J. Zhuchen, J. Arvay, J. Watt, J. T. Miller, A. Datye and F. H. Ribeiro, Catalytic Reactivity of Pt Sites for Non-Oxidative Coupling of Methane (NOCM), *Chem. Eng. J.*, 2024, **481**, 148675.

44 J. Lunsford, The Catalytic Conversion of Methane to Higher Hydrocarbons, *Catal. Today*, 1990, **6**(3), 235–259.

45 X. Guo, G. Fang, G. Li, H. Ma, H. Fan, L. Yu, C. Ma, X. Wu, D. Deng, M. Wei, D. Tan, R. Si, S. Zhang, J. Li, L. Sun, Z. Tang, X. Pan and X. Bao, Direct, Nonoxidative Conversion of Methane to Ethylene, Aromatics, and Hydrogen, *Science*, 2014, **344**(6184), 616–619.

46 S. Li, R. Cao, M. Xu, Y. Deng, L. Lin, S. Yao, X. Liang, M. Peng, Z. Gao, Y. Ge, J. X. Liu, W. X. Li, W. Zhou and D. Ma, Atomically Dispersed Ir/α-MoC Catalyst with High Metal Loading and Thermal Stability for Water-Promoted Hydrogenation Reaction, *Natl. Sci. Rev.*, 2022, **9**(1), nwab026.

47 L. V. Mattos, G. Jacobs, B. H. Davis and F. B. Noronha, Production of Hydrogen from Ethanol: Review of Reaction Mechanism and Catalyst Deactivation, *Chem. Rev.*, 2012, **112**(7), 4094–4123.

48 M. D. Argyle and C. H. Bartholomew, Heterogeneous Catalyst Deactivation and Regeneration: A Review, *Catalysts*, 2015, **5**, 145–269.

49 H. O. Otor, J. B. Steiner, C. Garcia-Sancho and A. C. Alba-Rubio, Encapsulation Methods for Control of Catalyst Deactivation: a Review, *ACS Catal.*, 2020, **10**(14), 7630–7656.

50 Y. Zhang and K. J. Smith, Carbon Formation Thresholds and Catalyst Deactivation During CH4 Decomposition on Supported Co and Ni Catalysts, *Catal. Lett.*, 2004, **95**(1), 7–12.

51 C. H. Tempelman and E. J. Hensen, On the Deactivation of Mo/HZSM-5 in the Methane Dehydroaromatization Reaction, *Appl. Catal., B*, 2015, **176–177**, 731–739.

52 Y. Song, Q. Zhang, Y. Xu, Y. Zhang, K. Matsuoka and Z. G. Zhang, Coke Accumulation and Deactivation Behavior of Microzeolite-Based Mo/HZSM-5 in the Non-Oxidative Methane Aromatization under Cyclic CH4-H2 Feed Switch Mode, *Appl. Catal., A*, 2017, **530**, 12–20.

53 A. J. Martin, S. Mitchell, C. Mondelli, S. Jaydev and J. Perez-Ramirez, Unifying Views on Catalyst Deactivation, *Nat. Catal.*, 2022, **5**, 845–866.

54 S. L. Scott, A Matter of Life(time) and Death, *ACS Catal.*, 2018, **8**(9), 8597–8599.

55 Q. Zhang, I. Lee, J. Ge, F. Zaera and Y. Yin, Surface-Protected Etching of Mesoporous Oxide Shells for the Stabilization of Metal Nanocatalysts, *Adv. Funct. Mater.*, 2010, **20**(14), 2201–2214.

56 V. Valtchev, G. Majano, S. Mintova and J. Perez-Ramirez, Tailored Crystalline Microporous Materials by Post-Synthesis Modification, *Chem. Soc. Rev.*, 2013, **42**, 263–290.

57 J. Peng, B. Chen, Z. Wang, J. Guo, B. Wu, S. Hao, Q. Zhang, L. Gu, Q. Zhou, Z. Liu, S. Hong, S. You, A. Fu, Z. Shi, H. Xie, D. Cao, C. J. Lin, G. Fu, L. S. Zheng, Y. Jiang and N. Zheng, Surface Coordination Layer Passivates Oxidation of Copper, *Nature*, 2020, **586**, 390–394.

58 G. Yaluris, R. Larson, J. Kobe, M. Gonzalez, K. Fogash and J. Dumesic, Selective Poisoning and Deactivation of Acid Sites on Sulfated Zirconia Catalysts Forn-Butane Isomerization, *J. Catal.*, 1996, **158**(1), 336–342.

59 T. J. Schwartz, S. D. Lyman, A. H. Motagamwala, M. A. Mellmer and J. A. Dumesic, Selective Hydrogenation of Unsaturated Carbon-Carbon Bonds in Aromatic-Containing Platform Molecules, *ACS Catal.*, 2016, **6**(3), 2047–2054.

60 D. Gerceker, A. H. Motagamwala, K. R. Rivera-Dones, J. B. Miller, G. W. Huber, M. Mavrikakis and J. A. Dumesic, Methane Conversion to Ethylene and Aromatics on PtSn Catalysts, *ACS Catal.*, 2017, **7**, 2088–2100.

61 S. Zhang, Z. Wu, X. Liu, Z. Shao, L. Xia, L. Zhong, H. Wang and Y. Sun, Tuning the Interaction between Na and Co2C to Promote Selective CO2 Hydrogenation to Ethanol, *Appl. Catal., B*, 2021, **293**, 120207.

62 Z. Li, L. Yu, C. Milligan, T. Ma, L. Zhou, Y. Cui, Z. Qi, N. Libretto, B. Xu, J. Luo, E. Shi, Z. Wu, H. Xin, W. N. Delgass, J. T. Miller and Y. Wu, Two-dimensional Transition Metal Carbides as Supports for Tuning the Chemistry of Catalytic Nanoparticles, *Nat. Commun.*, 2018, **9**, 5258.

63 Z. Li, Z. Qi, S. Wang, T. Ma, L. Zhou, Z. Wu, X. Luan, F. Y. Lin, M. Chen, J. T. Miller, H. Xin, W. Huang and Y. Wu, In Situ Formed Pt3Ti Nanoparticles on a Two-Dimensional Transition Metal Carbide (MXene) Used as Efficient Catalysts for Hydrogen Evolution Reactions, *Nano Lett.*, 2019, **19**(8), 5102–5108.

64 Z. Li, T. K. Misicko, F. Yang, X. Liu, Z. Wu, X. Gao, T. Ma, J. T. Miller, D. S. Mainardi, C. D. Wick, Z. Zeng, Y. Xiao and Y. Wu, Two-dimensional Atomically Thin Pt Layers on MXenes: the Role of Electronic Effects during Catalytic Dehydrogenation of Ethane and Propane, *Nano Res.*, 2024, **17**, 1251–1258.

65 Y. Xiao and A. Varma, Catalytic Deoxygenation of Guaiacol Using Methane, *ACS Sustainable Chem. Eng.*, 2015, **3**(11), 2606–2610.

66 Y. Xiao and A. Varma, Kinetics of Guaiacol Deoxygenation Using Methane over the Pt-Bi Catalyst, *React. Chem. Eng.*, 2017, **2**(1), 36–43.

67 Y. Xiao, J. Greeley, A. Varma, Z. J. Zhao and G. Xiao, An Experimental and Theoretical Study of Glycerol Oxidation to 1,3-Dihydroxyacetone over Bimetallic Pt-Bi Catalysts, *AIChE J.*, 2017, **63**(2), 705–715.

68 S. Roy, A. Cherevotan and S. C. Peter, Thermochemical CO2 Hydrogenation to Single Carbon Products: Scientific and Technological Challenges, *ACS Energy Lett.*, 2018, 1938–1966.

69 J. ZhuChen, Z. Wu, X. Zhang, S. Choi, Y. Xiao, A. Varma, W. Liu, G. Zhang and J. T. Miller, Identification of the Structure of the Bi Promoted Pt Non-oxidative Coupling of Methane Catalyst:a Nanoscale Pt3Bi Intermetallic Alloy, *Catal. Sci. Technol.*, 2019, **9**, 1349–1356.

70 H. F. Sheng and R. F. Lobo, Non-oxidative Coupling of Methane to Ethylene Using Mo2C/[B]ZSM-5, *ChemPhysChem*, 2018, **19**, 1–19.

71 K. Motokura, A. Mizuno, S. Hasegawa, M. Nambo, M. Takabatake, K. Suzuki, Y. Manaka, Y. Uemura, S. Tsubaki and W. J. Chun, In Situ Formation of Ru-Sn Bimetallic Particles for Nonoxidative Coupling of Methane, *J. Phys. Chem. C*, 2023, **127**(31), 15185–15194.

72 R. K. Grasselli, Site Isolation and Phase Cooperation: Two Important Concepts in Selective Oxidation Catalysis: a Retrospective, *Catal. Today*, 2014, **238**, 10–27.

73 T. Drake, P. Ji and W. Lin, Site Isolation in Metal-Organic Frameworks Enables Novel Transition Metal Catalysis, *Acc. Chem. Res.*, 2018, **51**(9), 2129–2138.

74 F. Yang, M. A. Hanna and R. Sun, Value-added Uses for Crude Glycerol–A Byproduct of Biodiesel Production, *Biotechnol. Biofuels*, 2012, **5**(1), 13.

75 J. Wang, X. Chen, C. Li, Y. Zhu, J. Li, S. Shan, A. Hunt, I. Waluyo, J. A. Boscoboinik, C. J. Zhong and G. Zhou, Tuning Strong Metal-Support Interactions via Synergistic Alloying, *ACS Catal.*, 2024, **14**(8), 5662–5674.

76 S. H. A. M. Leenders, R. Gramage-Doria, B. de Bruin and J. N. H. Reek, Transition Metal Catalysis in Confined Spaces, *Chem. Soc. Rev.*, 2015, **44**, 433–448.

77 Q. Fu and X. Bao, Surface Chemistry and Catalysis Confined under Two-Dimensional Materials, *Chem. Soc. Rev.*, 2017, **46**, 1842–1874.

78 T. A. Shifa and A. Vomiero, Confined Catalysis: Progress and Prospects in Energy Conversion, *Adv. Energy Mater.*, 2019, **9**(40), 1902307.

79 F. Bauer, W. H. Chen, H. Ernst, S. J. Huang, A. Freyer and S. B. Liu, Selectivity Improvement in Xylene Isomerization, *Microporous Mesoporous Mater.*, 2004, **72**(1), 81–89.

80 Y. Gan, Q. Lv, Y. Li, H. Yang, K. Xu, L. Wu, Y. Tang and L. Tan, Acidity Regulation for Improved Activity of Mo/HZSM-5 Catalyst in Methane Dehydroaromatization, *Chem. Eng. Sci.*, 2023, **266**, 118289.

81 C. H. Collett and J. McGregor, Things Go Better with Coke: the Beneficial Role of Carbonaceous Deposits in Heterogeneous Catalysis, *Catal. Sci. Technol.*, 2016, **6**, 363–378.

82 J. F. Haw, W. Song, D. M. Marcus and J. B. Nicholas, The Mechanism of Methanol to Hydrocarbon Catalysis, *Acc. Chem. Res.*, 2003, **36**(5), 317–326.

83 S. G. Sanz, L. McMillan, J. McGregor, J. A. Zeitler, N. Al-Yassir, S. Al-Khattaf and L. F. Gladden, The Enhancement of the Catalytic Performance of CrOx/Al02O3 Catalysts for Ethylbenzene Dehydrogenation through Tailored Coke Deposition, *Catal. Sci. Technol.*, 2016, **6**(4), 1120–1133.

84 J. J. Kromwijk, J. G. Vloedgraven, F. Neijenhuis, W. van der Stam, M. Monai and B. M. Weckhuysen, Impact of Tungsten Loading on the Activation of Zeolite-Based Catalysts for Methane Dehydroaromatization, *ACS Catal.*, 2025, **15**(9), 7241–7253.

85 F. Bauer, W. Chen, E. Bilz, A. Freyer, V. Sauerland and S. Liu, Surface Modification of Nano-Sized HZSM-5 and HFER by Pre-Coking and Silanization, *J. Catal.*, 2007, **251**(2), 258–270.

86 P. Losch, M. Boltz, C. Bernardon, B. Louis, A. Palčić and V. Valtchev, Impact of External Surface Passivation of Nano-ZSM-5 Zeolites in the Methanol-to-Olefins Reaction, *Appl. Catal., A*, 2016, **509**, 30–37.